

EVALUATION OF MODULUS AND POISSON'S RATIO FROM TRIAXIAL TESTS

M. Hassan Farzin, Stone and Webster Engineering Corporation, Boston; and
Raymond J. Krizek and Ross B. Corotis, Technological Institute,
Northwestern University

A method is suggested to determine piecewise linear, stress-dependent relationships for the modulus and Poisson's ratio of soils. The method is based on linear elasticity and conditions associated with conventional triaxial tests at different states of stress. The tangent modulus at a given stress level is shown to be the slope of the axial stress-axial strain curve at that stress level, and the value of Poisson's ratio is evaluated by use of theoretical considerations and a simple graphical construction. This method of interpretation is applied to experimental data from two natural soils used in an actual full-scale field installation of buried concrete pipe, and the results are shown to be in reasonable agreement with those determined by more sophisticated analyses and more extensive experimental measurements. It is also demonstrated that other analytical methods for interpreting these test data may yield significantly different values for the mechanical properties of soils, and this must be taken into account when such results are incorporated into mathematical models for the response of soil-structure systems.

•ONE of the major difficulties associated with currently available techniques of analysis for problems in soil-structure interaction is the specification of soil properties. Although high-speed digital computers and the finite element method have provided the opportunity to handle material properties in a more realistic manner, the determination of these properties has been the subject of much controversy. Several recent studies (4, 5, 6) have helped immensely in the understanding of soil behavior under complicated states of stress, but the tests discussed involve the use of sophisticated equipment that is generally not available in most laboratories. Therefore, there is still a pressing need for a procedure that can be used with data from a standard laboratory test to deduce the material properties required in the formulation of a problem involving soil response. Accordingly, this study will describe and evaluate experimentally a method that interprets the results of a conventional triaxial test to obtain piecewise linear values for the modulus and Poisson's ratio of soil.

STRESS-STRAIN PARAMETERS

The theoretical formulation of any problem based on the theories of piecewise linear elasticity requires two parameters, the modulus of elasticity E and Poisson's ratio ν , to characterize an isotropic material. By definition, E is the slope of the axial stress-axial strain curve in a uniaxial stress test, and ν is the ratio of the lateral strain to the longitudinal strain for a specimen that is uniaxially stressed in the longitudinal direction. The state of stress in both cases is assumed to be homogeneous. Since it is

generally not practical to test soil under homogeneous states of stress, three different and somewhat less ideal laboratory tests (uniaxial strain test, triaxial test, and plane strain test) are usually used; however, the results of these tests are generally interpreted on the basis that the soil specimen is an infinitesimal element with an associated homogeneous state of stress. This assumption is not true, and serious errors may be introduced because of the various boundary conditions. Accordingly, unless otherwise shown, none of the conventional soil tests can provide directly the values of E and ν for soils.

Even if the notion of an infinitesimal element and homogeneous state of stress is accepted, the usual test data (which do not include lateral deformation or lateral stress measurements) and method of interpretation allow the evaluation of only one parameter, especially for partially saturated soils. In such cases, ν is often assumed, and Hooke's law is used to determine E . For example, the results of a uniaxial strain test and an assumption for ν may be used in conjunction with

$$E = \frac{\sigma_1}{\epsilon_1} \left(1 - \frac{2\nu^2}{1-\nu} \right)$$

to determine E . However, the test is usually performed to determine the values of both parameters.

SCOPE OF STUDY

The theoretical part of this study considers the boundary value problem associated with a triaxial compression test on a cylindrical soil specimen, and the effect of the assumption of a homogeneous state of stress is evaluated. Results of the theoretical findings were verified experimentally by conducting triaxial tests with radial deformation measurements on two soils from an actual full-scale field installation of buried concrete pipe, and comparison was made with other methods for determining these parameters. Throughout this investigation, we assumed the soil to be isotropic, time-independent, and piecewise linear elastic and the loading to be monotonic.

THEORETICAL CONSIDERATIONS

For the boundary conditions usually associated with a conventional triaxial test with rough end platens, the radial and axial displacement components, u and w , of a linear elastic cylinder subjected to the axially symmetric loading conditions shown schematically in Figure 1 can be closely approximated by

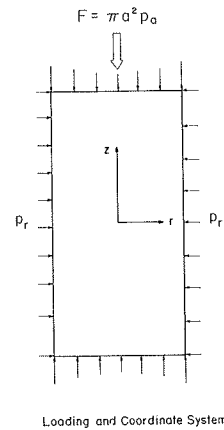
$$u = u_0 r + \frac{1}{3} u_1 r^3 + \frac{1}{5} u_2 r^5 + \frac{1}{2} u_3 r z^2 + \frac{1}{2} u_4 r^3 z^2 + \frac{1}{4} u_5 r z^4 + U \quad (1)$$

$$w = w_0 z + \frac{1}{3} w_1 z^3 + \frac{1}{5} w_2 z^5 + \frac{1}{2} w_3 r^2 z + \frac{1}{2} w_4 r^2 z^3 + \frac{1}{4} w_5 r^4 z + W \quad (2)$$

where the periodic parts U and W are given by

$$U = \sum_{n=1}^{\infty} \left[-\frac{A_n}{k} I_1(kr) - \frac{C}{k} r I_0(kr) \right] \cos kz \quad (3)$$

Figure 1. Test specimen and boundary conditions.



$$W = \sum_{n=1}^{\infty} \left[\frac{A_2}{K} I_0(kr) + \frac{C}{K} r I_1(kr) \right] \sin kz \quad (4)$$

in which $I_0(kr)$ and $I_1(kr)$ are Bessel functions of the zero and first order respectively, and kr is the imaginary argument. The derivation of equations 1, 2, 3, and 4 and the associated coefficients are given by Farzin, Corotis, and Krizek (3). An evaluation of the vertical displacement w at the ends ($z = \pm c$) of the specimen yields

$$w = w_0 c + \frac{1}{3} w_1 c^3 + \frac{1}{5} w_2 c^5 \quad (5)$$

The vertical displacement w can be shown to vary with z in essentially a linear manner; thus, the axial strain ϵ_a at any point in the middle three-quarters of the specimen may be defined as essentially w/c , and equation 5 may be reasonably written as

$$\epsilon_a = w_0 + \frac{1}{3} c^2 w_1 + \frac{1}{5} c^4 w_2 \quad (6)$$

where

$$w_0 = \frac{p_a}{E} \left\{ D \left[\frac{2g_1 + h_1(1 - 2\nu)}{2\nu} \right] - \frac{p_r}{p_a} \frac{1}{\nu} (1 + \nu) (1 - 2\nu) \right\} \quad (7)$$

$$w_1 = \frac{p_a}{a^2 E} D \frac{1}{2(1 - \nu)} \left(1 - \frac{8}{3} S^2 \right) \quad (8)$$

$$w_2 = \frac{2}{3} \frac{p_a}{a^4 E} D \left(\frac{1}{1 - \nu} \right) \quad (9)$$

in which

$$D = \frac{2(1 + \nu) \left[\frac{p_r}{p_a} (1 - \nu) - \nu \right]}{2g_1(1 + \nu) + \nu f_1 + h_1(1 - \nu)} \quad (10)$$

$$f_1 = \frac{\nu}{6(1-\nu)} + \frac{1}{3}S^2 - \frac{14}{45}\left(\frac{2-\nu}{1-\nu}\right)S^4 \quad (11)$$

$$g_1 = \frac{1}{12}\left[\frac{1-2\nu}{2(1-\nu)} - \delta\right] - \frac{1}{6}S^2 + \frac{1}{3}\left[\frac{3-2\nu}{2(1-\nu)} - \frac{4}{15}\left(\frac{2-\nu}{1-\nu}\right)\right]S^4 \quad (12)$$

$$h_1 = -\frac{7}{15}S^4\left(\frac{1}{1-\nu}\right) - \frac{1}{12}\left(\frac{2-\nu}{1-\nu}\right) + \frac{1}{3}S^2\left(\frac{1}{1-\nu}\right) \quad (13)$$

$$\delta = \sum_{n=1}^{\infty} \frac{24}{\alpha^3} \frac{\left[(2\gamma+1)\alpha + \frac{4}{\alpha}(8\gamma+1)\right] I_1^2 - (8\gamma+4) I_0 I_1}{\gamma\alpha^2 I_0^2 - (1+\gamma\alpha^2) I_1^2} \quad (14)$$

$$\gamma = \frac{1}{2(1-\nu)} \quad (15)$$

$$\alpha = ka \quad (16)$$

$$S = \frac{c}{a} \quad (17)$$

$$k = \frac{n\pi}{c} \quad (18)$$

where I_0 and I_1 are Bessel functions of the zero order respectively, α is the imaginary argument, and p_a is the average distributed axial load given by

$$p_a = \frac{1}{\pi a^2} \int_0^a \int_0^{2\pi} \sigma_z r dr d\theta \quad (19)$$

The rate of change of the axial strain ϵ_a for the average distributed axial load p_a can be determined by the differentiation of equation 6 with respect to p_a . The result is

$$\frac{d\epsilon_a}{dp_a} = \frac{dw_0}{dp_a} + \frac{1}{3}c^2 \frac{dw_1}{dp_a} + \frac{1}{5}c^4 \frac{dw_2}{dp_a} \quad (20)$$

Differentiation of equations 7, 8, and 9 gives

$$\frac{dw_0}{dp_a} = \frac{1}{E} \left\{ \frac{\left[\frac{2g_1 + h_1(1-2\nu)}{2\nu} \right] 2(1+\nu)(-\nu)}{2g_1(1+\nu) + \nu f_1 + h_1(1-\nu)} \right\} \quad (21)$$

$$\frac{dw_1}{dp_a} = \frac{1}{E} \left\{ \left(1 - \frac{8S^2}{3} \right) \frac{1}{2a^2(1-\nu)} \left[\frac{-2\nu(1+\nu)}{2g_1(1+\nu) + \nu f_1 + h_1(1-\nu)} \right] \right\} \quad (22)$$

$$\frac{dw_2}{dp_a} = \frac{1}{E} \left\{ \frac{2}{3} \left[\frac{1}{a^4(1-\nu)} \right] \left[\frac{-2\nu(1+\nu)}{2g_1(1+\nu) + \nu f_1 + h_1(1-\nu)} \right] \right\} \quad (23)$$

Since equations 21, 22, and 23 are independent of p_a , it follows that the slope given by equation 20 is also independent of p_a . When equations 21, 22, and 23 are substituted into equation 20, a long and tedious computation yields

$$\frac{d\epsilon_a}{dp_a} = \frac{A}{E} = \frac{1}{E_T} \quad (24)$$

where E_T is the slope of the axial stress versus axial strain measured in a conventional triaxial test, A is a function of Poisson's ratio ν , and the slenderness ratio S of the specimen is

$$A = (1 + \nu) \left[\frac{\frac{8}{45}(S^4 - \frac{\delta}{6}) - \frac{1}{12}(1 - 2\nu)}{(1 + \nu)\left(\frac{8}{45}S^4 - \frac{\delta}{6}\right) - \frac{1}{12}(1 - \nu)} \right] \quad (25)$$

in which δ is given by equation 14. When equation 24 is rewritten as

$$E = A \frac{dp_a}{d\epsilon_a} = AE_T \quad (26)$$

it can be seen on Figure 2a that A approaches unity, or E approaches E_T , as S increases. In particular, for values of 0.3 or 0.4 for Poisson's ratio, the error is on the order of 4 to 6 percent at a slenderness ratio of 2 (commonly used for triaxial test specimens). However, since the actual boundary conditions at the ends of the specimen may be somewhat less constrained than the idealized rough boundary conditions assumed in this solution, the actual error may be slightly less. For small values of S , the value of A from equation 25 is such that E_T approaches the constrained modulus M (Figure 2b).

The preceding results can also be shown by direct algebraic computation. For example, if large values ($S > 2$) are assumed for the slenderness ratio S , α is small, and the ratio of I_0/I_1 can be approximated by

$$I_0/I_1 = \frac{2}{\alpha} \left(1 + \frac{\alpha^2}{8} - \frac{\alpha^4}{192} + \dots \right) \quad (27)$$

Retention of terms up to the fourth order and direct substitution of equation 27 into equation 14 give

$$\delta = 96 \sum_{n=1}^{\infty} \frac{1}{\alpha^4} \left\{ 1 + \frac{\alpha^4}{96} \left[\frac{23 + 24(1 - \nu)}{2(1 + \nu)} \right] \right\} \quad (28)$$

which, on expansion and retention of only the fourth order terms, becomes

$$\delta = \frac{96}{90} S^4 + m \frac{23 + 24(1 - \nu)}{2(1 + \nu)} \quad (29)$$

where π^4 is approximated by 90, and m is the largest number of terms taken in equation 28 for which the approximation given by equation 27 (small α , where $\alpha = m\pi/S$) is acceptable. Substitution of the values for δ given by equation 29 into equation 24 yields

$$\frac{d\epsilon_a}{dp_a} = \frac{1}{E} \left(\frac{-\frac{1}{2}[23 + 24(1 - \nu)]m - \frac{1}{12}(1 - 2\nu)(1 + \nu)}{-\frac{1}{2}[23 + 24(1 - \nu)]m - \frac{1}{12}(1 - \nu)} \right) \quad (30)$$

Since, for small values of α , the first terms in both the numerator and the denominator of the right side of equation 30 are large relative to the other terms, they dominate the magnitude of equation 30. Thus, for a long specimen ($S \geq 2$), equation 30 can be approximated by

$$E_r = \frac{dp_a}{d\epsilon_a} \approx E \quad (31)$$

Implicit in the conclusion that E approaches $dp_a/d\epsilon_a$ as S increases is the suggestion that the radial deformations u are approximately uniform over most of the length of the specimen. As shown in Figure 3 for three typical cases, this is indeed true from a theoretical point of view. For purposes of emphasis, the scale of the deformations is different from that used for the dimensions of the specimen. In the middle case, the applied pressures and the value of Poisson's ratio are such that the radial deformations are almost zero.

Letting

$$p_a = mp_r \quad (32)$$

and

$$\epsilon_a = \beta p_r \quad (33)$$

equation 6 can be plotted conveniently, as in Figure 4, in terms of generalized parameters p_a/p_r , βp_r , and Poisson's ratio ν . As previously explained, the influence of S is negligible if $S \geq 2$. It is observed that the ordinate of the point where the plot intersects the axial pressure axis is directly proportional to the value of Poisson's ratio. This characteristic can be used advantageously to determine the value of Poisson's

Figure 2. Variation of moduli versus slenderness ratio.

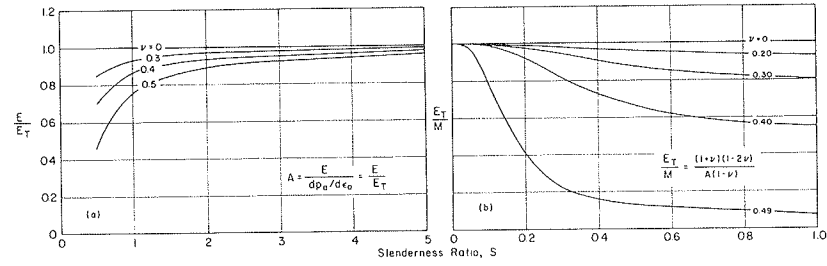


Figure 3. Radial deformations along specimen.

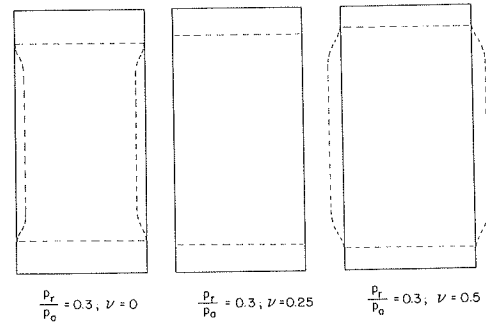


Figure 4. Idealized relationships among pressure, strain, and elastic properties.

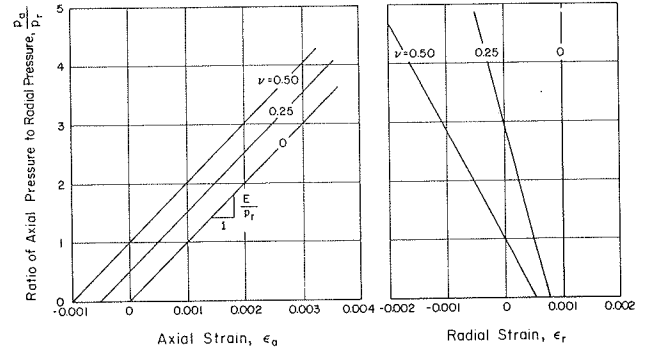
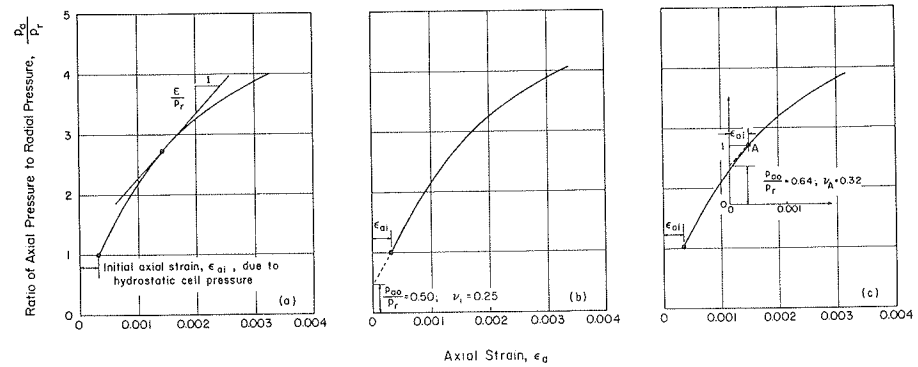


Figure 5. Stepwise determination of linear elastic properties from experimental data.



ratio from the results of a conventional triaxial test in which only the axial displacement of the specimen is measured. This is accomplished by setting ϵ_a equal to zero and by combining equations 6, 7, 8, and 9 to obtain

$$\frac{p_a}{p_r} = \frac{A - (1 + \nu) \left(\frac{1 - 2\nu}{1 - \nu} \right)}{A \left(\frac{\nu}{1 - \nu} \right)} \quad (34)$$

For $S \geq 2$, $A \approx 1$ and equation 34 reduces to

$$\frac{p_a}{p_r} = 2\nu \quad (35)$$

Hence, if p_a/p_r is known to be $\epsilon_a = 0$, ν may be readily determined from equation 35.

EVALUATION OF MATERIAL PROPERTIES

Modulus

As shown by equation 31, the value of E at a given stress level can be evaluated by taking the slope of the axial stress-axial strain curve, which is obtained from a conventional triaxial test with a constant cell pressure. Such a curve is shown in Figure 5a. These values of moduli are termed tangent moduli since they characterize a change in loading in terms of a series of incremental loads.

Poisson's Ratio

Equation 35 shows that, if the value of the axial pressure p_{a0} is given at $\epsilon_a = 0$, the initial value of Poisson's ratio can be readily calculated. As shown in Figure 5b, the value of p_{a0} can be determined by measuring the initial axial strain ϵ_{a1} of the soil specimen due to the hydrostatic cell pressure and by extending the experimental stress-strain curve to the stress axis. This latter extension, if a straight-line segment is used, corresponds to the assumption of linear soil properties under the action of the cell pressure alone. Although radial displacements were not measured directly as the cell pressure was applied because of changes in the cell diameter (and thereby the reference datum for the radial displacement measurements), the initial radial strain ϵ_{r1} due to the hydrostatic cell pressure is assumed to be equal to ϵ_{a1} . Therefore, plots of both axial strain and radial strain versus axial pressure begin at the point $(\epsilon_{a1} = \epsilon_{r1}, p_{a0})$.

The tangent value of Poisson's ratio at any other point A along an actual stress-strain curve can be determined in a manner similar to that previously described by establishing a new coordinate system parallel to the original one. To position this new coordinate system, one may conveniently assume that point A has the coordinates $(\epsilon_{a1}, 1)$ in the new system. In effect, this implies that the bulk modulus of the soil does not vary with the state of stress. Although this is not strictly correct, the stress levels of interest are relatively low. [The maximum axial stress is on the order of 50 psi (345 kPa) and thereby tends to minimize the anticipated stiffening of a soil as stress increases. The relationship $K = E/[3(1 - 2\nu)]$ qualitatively favors such an assumption because the modulus decreases and Poisson's ratio increases as the axial stress is increased in a triaxial test. This causes both the numerator and denominator to decrease simultaneously, but not necessarily proportionately.] Within the limitation of this

assumption, the intercept on the new vertical axis of a straight line drawn tangent to point A will yield twice the tangent value of Poisson's ratio at point A, as shown in Figure 5c.

EXPERIMENTAL INVESTIGATION

To evaluate the foregoing theory, we conducted triaxial tests on two soils with radial and axial displacement measurements at several boundary points. Soil EB-1 is a mixture of coarse to very fine sand and gravel. Of material passing a No. 8 sieve, about 95 percent was sand and about 5 percent was silt. Soil EC-1 is a mixture of sand, silt, and clay. Of material passing a No. 8 sieve, about 40 percent was sand, 35 percent was silt, and 25 percent was clay. One specimen of each soil was tested under a constant confining pressure of 10 psi (69 kPa), and typical data from two tests are given in Figure 6. Measured radial displacements near the ends of the specimens confirmed the assumption of essentially zero radial expansion at the soil-platen interface.

The values of E and ν shown in Figure 7 were determined by the method described, which uses only axial displacement measurements, and by the inverse method (3), which uses both axial and radial displacement measurements. Also included are values of Poisson's ratio calculated as a simple ratio of the increment of radial strain, measured from ϵ_{rt} , to the increment of axial strain, measured from ϵ_{at} , and there is no adjustment for the fact that the test involves a triaxial, rather than a uniaxial, state of stress. For small-strain, monotonic-loading, time-independent, and drained conditions, the agreement between the first two methods and the ratio of radial to axial strain taken as Poisson's ratio is good. It appears reasonable to use the theory of elasticity to characterize soil behavior in a piecewise linear manner. Although a comparison of these ν values with values determined by some other method (2) would have been desirable, this test program was not sufficiently comprehensive to facilitate this comparison. Values for E , however, were determined by the method described by Duncan and Chang (1) and are shown in Figure 7. The method used to interpret data from a laboratory test can make significant differences in the resulting mechanical properties, and this fact must be fully appreciated when such results are incorporated into mathematical models. Since the values of Poisson's ratio are greatly affected by the initial axial strain due to the cell pressure, extreme care must be exercised to ensure that the initial displacement has been measured accurately and does not include seating errors or errors due to the expansion of the cell itself when pressured to p_c .

DISCUSSION OF RESULTS

The foregoing method describes a relatively straightforward means for interpreting data from a conventional triaxial compression test and for determining E and ν values that are consistent with the use of a piecewise linear elastic relation for formulating problems in soil-structure interaction. Modulus values are often calculated by use of several oversimplified procedures in which the soil specimen is treated as an infinitesimal element subjected to a given state of stress and the actual boundary conditions of the test specimen are not incorporated into the analysis. For the simplest of these approaches the tangent modulus is defined as

$$E = \frac{\Delta p_a}{\Delta \epsilon_a} \quad (36)$$

Although strictly incorrect because it represents the ratio of shear stress to normal strain, an analogous modulus sometimes used in mathematical models is defined as

Figure 6. Load-deformation data from triaxial test.

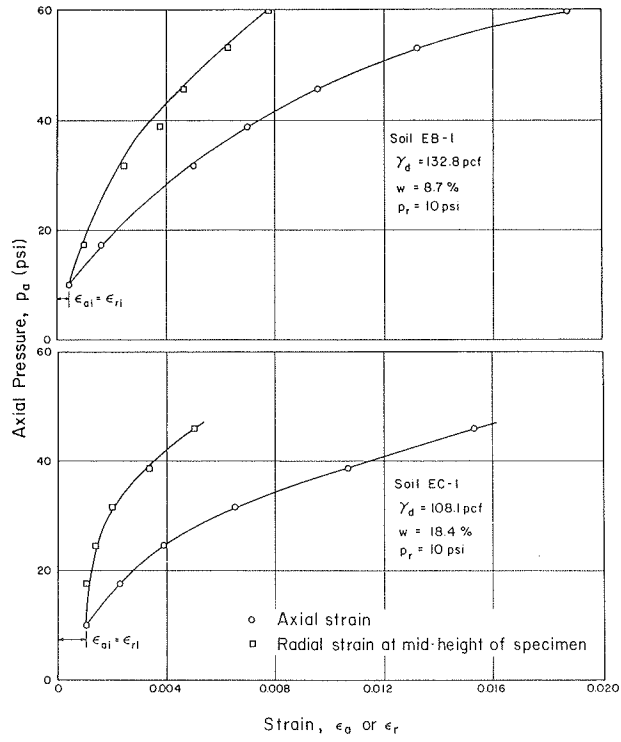
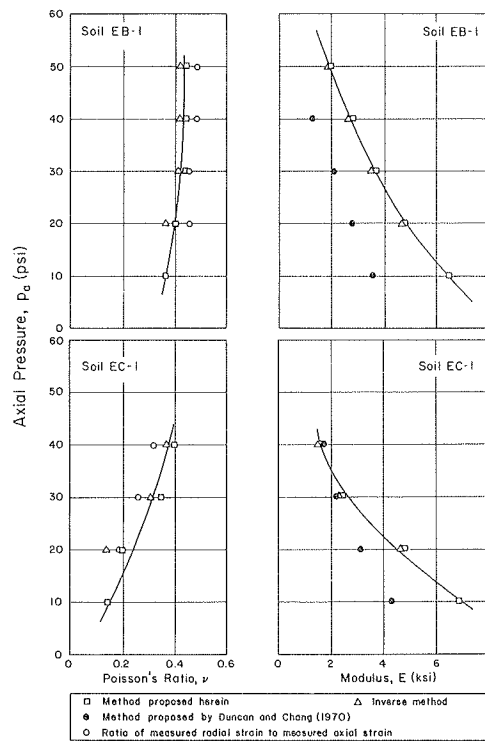


Figure 7. Modulus and Poisson's ratio versus axial pressure for soils EB-1 and EC-1.



$$E = \frac{\Delta(p_a - p_r)}{\Delta\epsilon_a} \quad (37)$$

In equations 36 and 37, p_a and p_r are usually termed the principal stresses σ_1 and σ_3 respectively. For the often encountered case in which p_r is maintained constant during the test, equations 36 and 37 are identical, and both are essentially the same as equation 31. However, there is a fundamental difference between equations 36 and 37 and equation 31 because a homogeneous state of stress has not been assumed to derive equation 31. Rather, the solution of the boundary value problem used and the conditions under which equation 31 is reasonably correct are evaluated. Similar reasoning applies to the determination of Poisson's ratio. For an idealized infinitesimal element of a linear elastic material subjected to a state of stress given by $\sigma_1 > \sigma_2 = \sigma_3$, one may write

$$\epsilon_1 = \frac{\sigma_1}{E} - \frac{2\nu\sigma_3}{E} \quad (38)$$

which, on setting $\epsilon_1 = 0$, becomes

$$\frac{\sigma_1}{\sigma_3} = 2\nu \quad (39)$$

Equation 39 is the same as equation 35, except that the latter was deduced by considering the actual test specimen and its associated boundary conditions. However, the graphical method shown in Figure 5 to determine stress-dependent values of Poisson's ratio has not generally been recognized heretofore.

CONCLUSIONS

Data from a standard triaxial compression test with no volume change measurements and no radial strain measurements can be used to determine piecewise linear values of the modulus and Poisson's ratio for a soil. The tangent modulus at a given stress level can be simply taken as the slope of the axial stress-axial strain curve at that stress level, and the value for Poisson's ratio can be evaluated by use of concepts from the theory of elasticity and some simple graphical constructions. Based on test data from two different soils, results deduced by this method are shown to be in reasonable agreement with results determined by more sophisticated analyses and by more extensive experimental measurements. Other methods for interpreting these data may yield significantly different values for the mechanical properties of the soil, and this must be taken into account when such results are incorporated into mathematical models for the response of soil-structure systems.

ACKNOWLEDGMENT

This work was performed in connection with a project supported by the American Concrete Pipe Association to investigate the soil-structure interaction of buried concrete pipe.

REFERENCES

1. J. M. Duncan and C. Y. Chang. Nonlinear Analysis of Stress and Strain in Soils. *Journal, Soil Mechanics and Foundations Division, American Society of Civil Engineers*, Vol. 96, No. SM5, 1970, pp. 1629-1653.
2. F. H. Kulhawy and J. M. Duncan. Stresses and Movements in Oroville Dam. *Journal, Soil Mechanics and Foundations Division, American Society of Civil Engineers*, Vol. 98, No. SM7, 1972, pp. 653-665.
3. M. H. Farzin, R. B. Corotis, and R. J. Krizek. Inverse Method for Determining Approximate Stress-Strain Behavior of Soils. *Journal of Testing and Evaluation, American Society for Testing and Materials*, 1974.
4. H. H. Roscoe. The Influence of Strains in Soil Mechanics. *Geotechnique*, Vol. 20, No. 2, 1970, pp. 129-170.
5. H. Y. Ko and R. F. Scott. A New Soil Testing Apparatus. *Geotechnique*, Vol. 17, 1967, pp. 40-57.
6. R. N. Yong and E. McKyes. Yield and Failure of Clay Under Triaxial Stresses. *Journal, Soil Mechanics and Foundations Division, American Society of Civil Engineers*, Vol. 97, No. SM1, 1971, pp. 159-176.